Inorganic Chemistry

Article

pubs.acs.org/IC

From Sequential to One-Pot Synthesis of Dipyrrin Based Grid-Type Mixed Metal–Organic Frameworks

Antoine Béziau, Stéphane A. Baudron,* Audrey Fluck, and Mir Wais Hosseini*

Laboratoire de Tectonique Moléculaire, UMR UdS-CNRS 7140, icFRC, Université de Strasbourg, F-67000, Strasbourg, France

Supporting Information

ABSTRACT: Both sequential and one-pot strategies for the preparation of a series of grid-type mixed metal–organic frameworks (MM′MOFs) based on dipyrrin ligands appended with either a pyridyl or a phenyl-imidazolyl moiety have been investigated. For the stepwise approach, the differentiation between the two coordination sites (nature, charge, and denticity) was exploited for the synthesis of a family of five discrete Zn(II), Cu(II), and Pd(II) complexes. Acting as metallatectons, these construction building blocks lead to the formation of a series of MM′MOFs upon self-assembly with $CdCl_2$. In these rhombic grid-type architectures, four consecutive metallatectons are bridged by Cd(II) cations adopting an octahedral coordination geometry with the chloride anions occupying apical positions, thus behaving as square nodes. The shape of the rhombus grids as well as the way they are packed (stacking or interpenetration) in the crystalline phase are controlled by the nature of metallatectons and the solvent molecules present in the crystals. Consequently, the heterometallic assemblies display different accessible voids, although they are built on layers with the same connectivity. More interestingly, as demonstrated by X-ray diffraction on both single crystals and microcrystalline powders, the same MM′MOFs were obtained by a one-pot strategy through direct combinations of dipyrrin derivatives with the corresponding metal salts. This one-pot approach is efficient and more convenient than the sequential alternative, since the isolation, purification, and characterization of the, sometimes insoluble, metallatectons are not required.

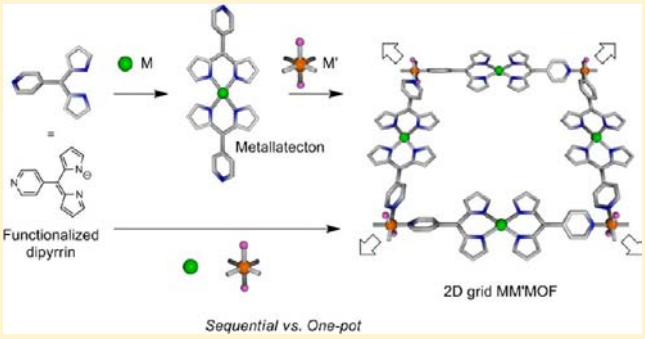

INTRODUCTION

Metal–organic frameworks (MOFs) and coordination polymers (CPs) have emerged, over the past two decades, as a novel class of crystalline hybrid materials with applications in separation, storage, and catalysis, for example.[1] The construction of these architectures is based on the self-assembly of polytopic organic ligands or tectons[2] with metal centers or metal complexes. Whereas, for homometallic systems, the direct one-pot combinations of organic and inorganic components may lead to the formation of the desired MOFs, the analogous reaction using different metal cations may also lead to diverse assemblies such as homometallic species and heterometallic ones featuring a random distribution of the metal centers (substitutional alloys). In order to circumvent this issue, a stepwise strategy based on organic tectons offering differentiated coordination sites has been developed for the formation of mixed metal–organic frameworks (MM′MOFs) with precise control of the location of the two metal centers (Figure 1, top).[3] Such derivatives form, upon reaction with a first metal center, a complex bearing peripheral coordinating sites that may be regarded as a metalloligand or metallatecton. Subsequent reaction of these species with secondary metal cations leads to the formation of MM′MOFs, for which both the distribution (ratio of M/M′) and location of metal centers within the architecture is preprogrammed and controlled by

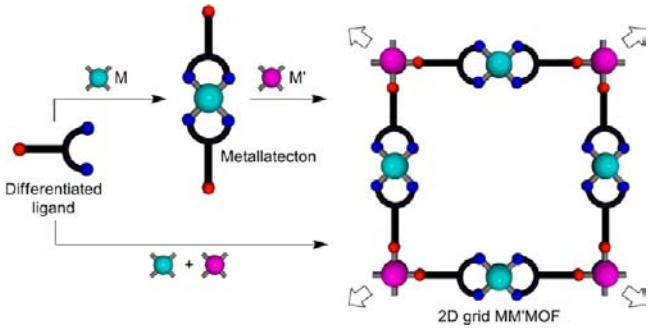

Figure 1. Sequential (top) and one-pot (bottom) strategies for the preparation of grid-type MM′MOFs based on a tecton offering differentiated coordination sites and two different metal centers M and M′.

both the design of the organic ligand (nature and location of the coordinating poles) and the choice of the metal center or metal complex (coordination geometry, number, and location of vacant coordination sites).

While this strategy has proven rather successful to prepare MM′MOFs,[3] it seems of interest to develop a direct one-pot

Received: November 21, 2013
Published: December 3, 2013

   dx.doi.org/10.1021/ic402892f | Inorg. Chem. 2013, 52, 14439–14448

Scheme 1. Representations of Dipyrrin, Ligands 1 and 2, and Metallatectons 3−7 Used for the Preparation of MCdMOFs 8−13

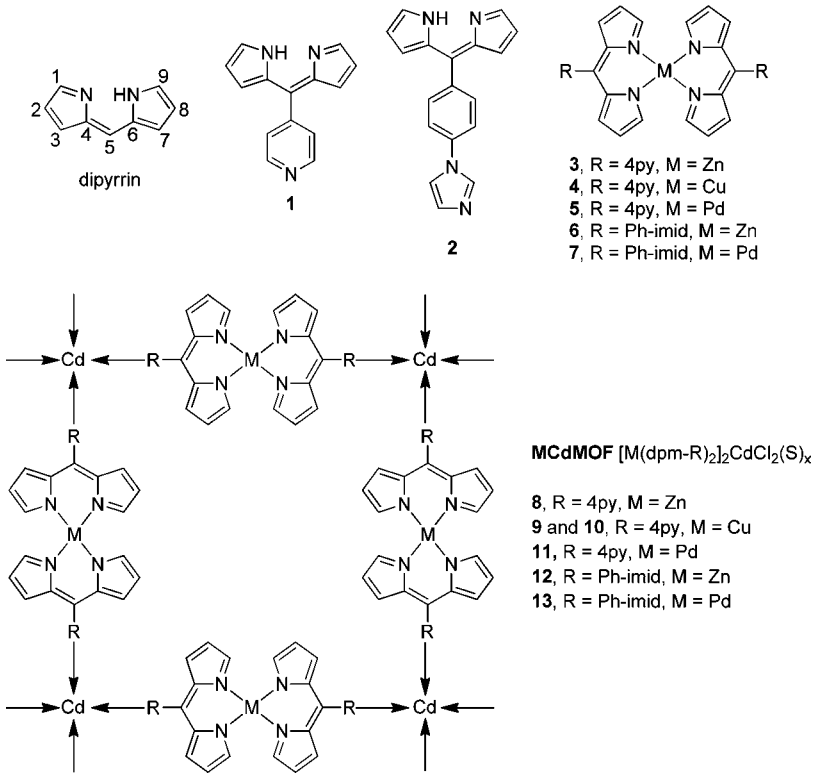

approach using mild conditions (Figure 1, bottom). However, in order to avoid scrambling and thus the random distribution of metal centers within the extended network, this strategy requires the design of organic tectons equipped with differentiated coordination sites with fine-tuning of their coordination propensity toward metal cations M and M′. To the best of our knowledge, this approach has not been explored for the room-temperature synthesis of MM′MOFs (nonsolvothermal conditions).

Dipyrrin[4] (dpm, Scheme 1), a bis-pyrrolic derivative forming a monoanionic chelate under mild alkaline conditions, may be readily appended with a peripheral coordinating unit leading thus to a ditopic ligand offering two coordination sites. The latter can be differentiated by their denticity (chelate vs monodentate) and charge (monoanionic vs neutral). This feature has been successfully exploited for the preparation of MM′MOFs, albeit solely following a sequential synthetic strategy. In almost all of these MM′MOFs, silver(I) cation as the secondary metal cation (M′) is combined with nitrile, pyridyl, or imidazolyl appended dpm based metallatectons.[5−7] However, it should be noted that Ag^+ cations also assemble with these complexes *via* Ag−π interactions with C=C bonds of the pyrrolic system, thus yielding complex architectures with a low degree of predictability.[6] Recently, we have described the sequential construction of grid-type heterobimetallic MM′MOFs (Figure 1, top) by combining Cd(II) salts with the homoleptic imidazole-appended Cu(II) metallatecton using ligand **2** (Scheme 1).[7] Cadmium salts were chosen as the secondary metal source given their known propensity to form homo- and heterometallic MOFs with bis-pyridine or bis-imidazolyl based ligands and metallatectons.[8,9] Indeed, the Cd(II) cation adopts an octahedral coordination geometry with two chloride anions occupying the axial positions, leading to a square neutral assembling node offering four available coordination sites which are occupied by four nitrogen atoms belonging to consecutive tectons. This initial result appeared as an interesting starting point for the generation of a larger family of MM′MOFs using other primary metal cations (M) and dipyrrins. Furthermore, as emphasized above, taking advantage of the differentiation of the two coordination sites, the synthesis of the same grid-type coordination polymers can be envisioned either by the stepwise strategy or by the proposed one-pot approach. We report herein an investigation demonstrating that the same heterometallic coordination networks may indeed be obtained efficiently through both sequential and one-pot strategies upon combining dpms **1** and **2** and Pd(II), Cu(II), or Zn(II) cations as M and Cd(II) as M′.

RESULTS AND DISCUSSION

The choice of combinations reported here is based on the modulation of both the organic tectons and M metal centers in order to vary not only the structural features of the extended 2D networks (geometry and packing of grid-type architectures) but also the solid state properties of the crystalline materials such as porosity and luminescence.

Synthesis and Crystal Structure of the Metallatectons. Dipyrrins **1** and **2** were synthesized as described.[5d,6c,10] The Pd(II), Cu(II), and Zn(II) metallatectons **3**−**7** (Scheme 1) were obtained in 70−90% yield by reaction of metal acetate or chloride salts with the corresponding dipyrrins, following reported literature procedures for such species.[11−13] Whereas compounds **3** and **4** were already described,[11,12] complexes **5**−**7** were unknown and have been characterized by mass spectrometry, UV−visible, and NMR spectroscopy. It should be noted that the Pd derivatives **5** and **7** are only sparingly soluble in common organic solvents.

The crystal structures of the five metallatectons have been determined by X-ray diffraction (Figure 2, Table 2). In the two

dx.doi.org/10.1021/ic402892f | Inorg. Chem. 2013, 52, 14439−14448

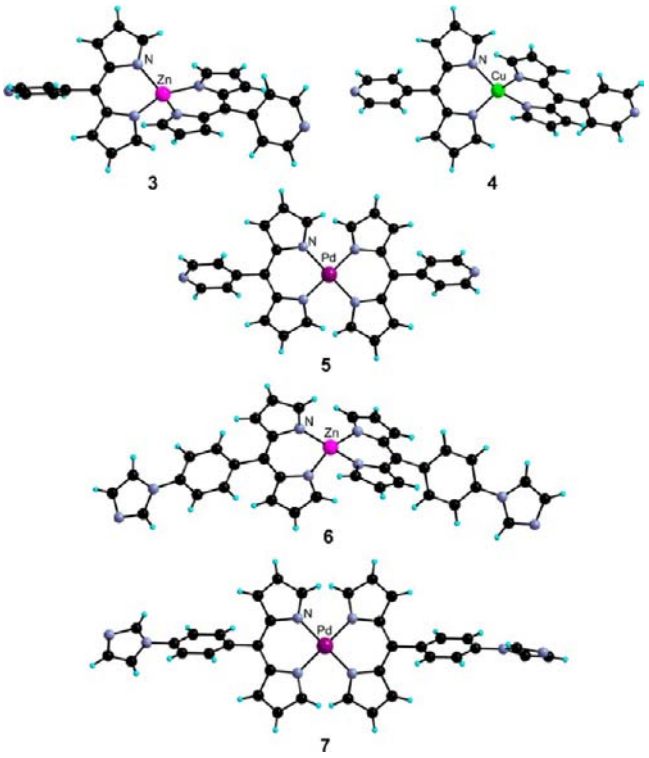

Figure 2. Crystal structures of complexes **3**–**7**. Solvent molecules have been omitted for clarity. Note that, for compound **7**, only one of the disordered imidazolyl groups is presented.

Table 1. Selected Average Distances (Å) for Compounds 3–13

	M	M-N	Cd–N	Cd–Cl	Cd---Cd
3	Zn	1.986			
8	Zn	1.979	2.370	2.593	20.013
4	Cu	1.968			
9	Cu	1.951	2.383	2.566	20.063
10	Cu	1.950	2.422	2.578	20.216
5	Pd	2.009			
11	Pd	2.009	2.392	2.579	19.858
6	Zn	1.976			
12	Zn	1.974	2.318	2.671	26.499
7	Pd	2.006			
13	Pd	2.021	2.318	2.630	25.303

Zn complexes, the metal cation adopts a slightly distorted tetrahedral coordination environment with C_5–Zn–$C_{5'}$ angles of 158.6 and 158.1° for **3** and **6**, respectively, and with Zn–N distances similar to what has been reported for analogous species (Table 1).[6a,11b,14] This distortion, probably due to packing effects, has also been observed in the structure of nonsolvated **3** and its mesityl-appended analogue.[11b] For complex **4** (Figure 2), the Cu(II) cation adopts a pseudotetrahedral coordination environment with bond distances and angles similar to the ones reported for a polymorphic structure (Table 1).[12,14,15] For complexes **5** and **7**, the Pd(II) is in a square-planar arrangement (Figure 2). Owing to the repulsion between C–H_α of the two dpms,[13,16] the pyrrolic rings are not coplanar within a chelate (29.5 and 36.0° for the two crystallographically independent complexes in **5**, 35.9° for **7**), unlike the Zn(II) and Cu(II) species. In the course of the investigation, the crystal structures of two solvates, $(\mathbf{5})(MeOH)_2$ and $(\mathbf{5})(CHCl_3)_2$, have also been obtained and are presented in the Supporting Information (Table S1 and Figure S1). As expected for Pd(II) complexes, they crystallize as discrete species and do not form self-assembled coordination polymers, unlike their recently reported Ni(II) analogues.[17]

Sequential Construction of Grid-Type MM′MOFs. MCdMOFs **8**–**13** of the $[M(dpm)_2]_2CdCl_2(solvent)_x$ type were prepared by diffusion of a MeOH solution of $CdCl_2$ into a solution of the corresponding preformed metallatecton in DMF, $CHCl_3$, or CH_2Cl_2 and characterized by single crystal X-ray diffraction. Let us examine first the architectures based on the pyridyl-appended dipyrrin **1**. Single crystals of ZnCdMOF **8** combining Zn(II) and Cd(II) metal centers ($[\mathbf{3}]_2CdCl_2$, Figure 3, left) were obtained using a DMF solution of the Zn(II) complex **3**. The same reaction with the Cu(II) analogue leading to the formation of CuCdMOF **9** ($[\mathbf{4}]_2CdCl_2$, Figure 3, middle), required vapor diffusion of Et_2O into the DMF/MeOH mixture. Owing to the important disorder of solvent molecules (DMF, MeOH, H_2O) for both structures, the corresponding electron density was removed using the SQUEEZE command.[18] In order to investigate the effect of solvent on the structural arrangement, a CH_2Cl_2/MeOH mixture was used instead, yielding crystals of compound **10** ($[\mathbf{4}]_2CdCl_2(CH_2Cl_2)_8$, Figure S2). Only the structure of **9** will be discussed in detail hereafter. Reaction of the Pd(II) metallatecton in $CHCl_3$ led to the formation of **11** ($[\mathbf{5}]_2CdCl_2(CHCl_3)_4$, Figure 3, right). In all four compounds, the Cd(II) cation is in an octahedral coordination environment with two chloride anions occupying the apical positions and four pyridyl groups belonging to four metallatectons in the square base (Figure 3). As expected, this leads to the formation of grid-type 2-D networks where the Cd(II) cations serving as connecting nodes are separated by *ca.* 20 Å (Table 1). While the connectivity is the same for the four grids, differences arise owing to the varying nature of the M(II) center of the metallatecton. In particular, for the Zn and Cu based systems, square grids are observed as a result of their tetragonal symmetry (Table 2) and the linear nature of the bridging complex (Figure 3). In this respect, it is worth noting that, unlike what is observed in the structure of **3**, the Zn(II) cation is in a perfectly tetrahedral coordination environment in **8** with a C_5–Zn–$C_{5'}$ angle of 180°. In contrast, rhombic grids are observed in PdCdMOF **11**. This is related to the distortion of the dpm chelate around the Pd(II) center, as seen in the structure of the discrete complex **5** (Figures 2 and 3). The pyrrolic rings within a dpm unit form an angle ranging from 31.5 to 34.1°. Therefore, whereas the 2D networks are flat in **8**–**10**, a ruffled arrangement is observed for **11** (Figure 3).

According to the proposed construction strategy (Figure 1), the design of the ligands and the resulting metallatectons and their combinations with Cd(II) halide direct the formation of 2-D networks. However, the way these grids organize in the crystal is not predetermined and results from the best packing of the sheet type architectures (Figure 4). The packing of 2-D networks leading to the formation of the crystal may be achieved either through stacking in an eclipsed or staggered manner or through interpenetration. This 3-D organization depends on the nature of M and M′, the dpm based tecton, and the solvent system used. Although for compounds **8**–**11**, based on the pyridyl appended dpm tecton **1**, no interpenetration is observed, different types of stacking are observed depending on the nature of the metal used to generate the metallatecton (Zn,

dx.doi.org/10.1021/ic402892f | *Inorg. Chem.* 2013, 52, 14439–14448

Table 2. Crystallographic Data for Complexes 3−7

	$3(\text{Dioxane})_{1/2}$	**4**	**5**	$(\mathbf{6})_2(Et_2O)$	**7**
formula	$C_{30}H_{24}N_6OZn$	$C_{28}H_{20}CuN_6$	$C_{28}H_{20}N_6Pd$	$C_{76}H_{62}N_{16}OZn_2$	$C_{36}H_{26}N_8Pd$
fw	549.95	504.04	546.90	1346.22	677.05
cryst syst	monoclinic	monoclinic	monoclinic	monoclinic	monoclinic
space group	$P2_1/c$	$P2_1/c$	$P2_1/c$	$P2_1/n$	$P2_1/c$
a, Å	14.7677(4)	13.6990(4)	8.6333(2)	18.0754(9)	12.0251(5)
b, Å	8.5971(2)	8.9494(3)	15.8070(3)	8.9756(3)	13.1586(5)
c, Å	20.3458(5)	19.4160(7)	16.6992(3)	20.8164(10)	9.0323(4)
β, deg	90.9300(10)	110.6360(10)	97.9620(10)	107.722(2)	94.580(2)
V, Å^3	2582.75(11)	2227.63(13)	2256.91(8)	3216.9(2)	1424.65(10)
Z	4	4	4	2	2
T, K	173(2)	173(2)	173(2)	173(2)	173(2)
μ, mm^{-1}	0.987	1.011	0.853	0.807	0.694
reflns. coll.	80878	35497	60455	31971	26423
ind. reflns. (R_{int})	7538 (0.0317)	6517 (0.0424)	6391 (0.0314)	9118 (0.0813)	3871 (0.0429)
R_1 ($I > 2\sigma(I)$)[a]	0.0345	0.0321	0.0248	0.0823	0.0421
wR_2 ($I > 2\sigma(I)$)[a]	0.0956	0.0898	0.0590	0.2119	0.1124
R_1 (all data)[a]	0.0473	0.0420	0.0397	0.1376	0.0758
wR_2 (all data)[a]	0.1071	0.0956	0.0685	0.2425	0.1468
GOF	1.081	1.066	1.028	1.134	1.091

[a] $R_1 = \sum||F_o| - |F_c||/\sum|F_o|$; $wR_2 = [\sum w(F_o^2 - F_c^2)^2/\sum wF_o^4]^{1/2}$.

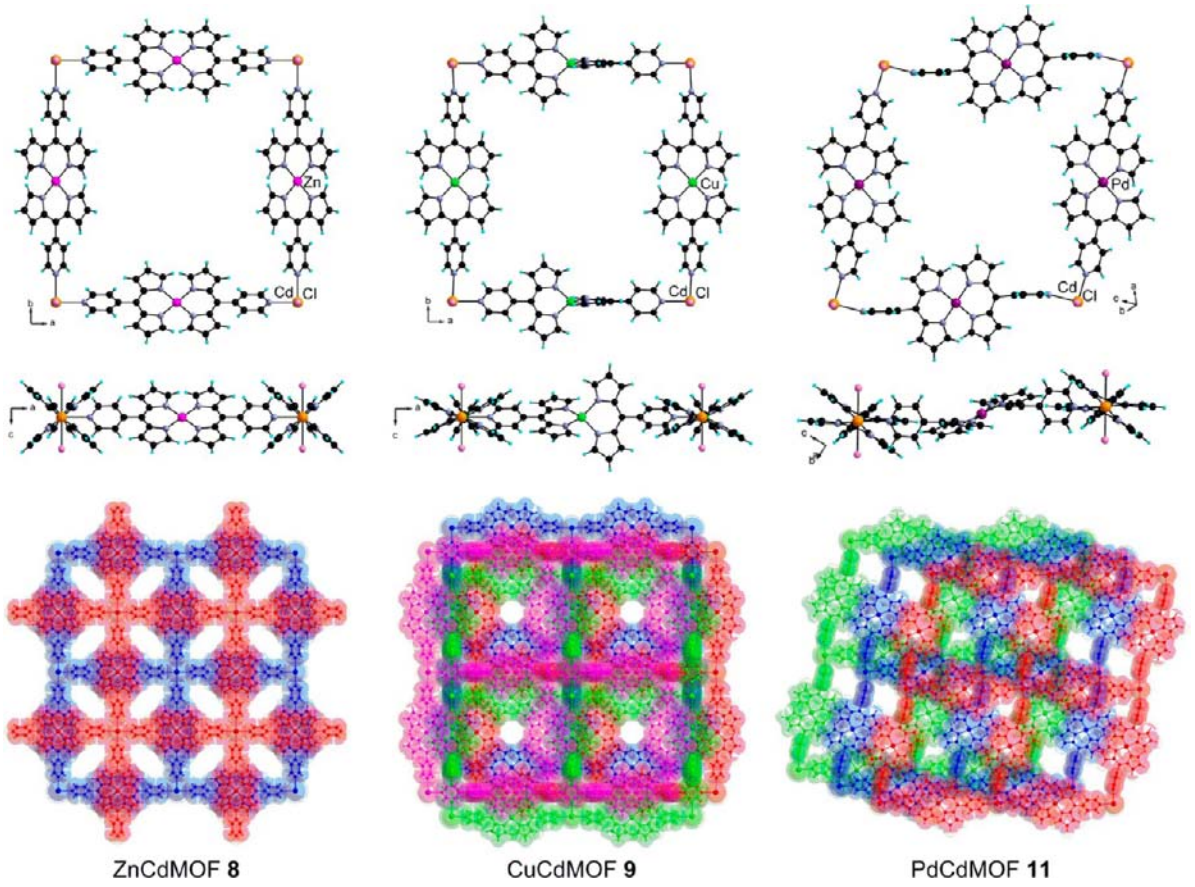

Figure 3. Portions of crystal structure of MCdMOFs **8**, **9**, and **11**. Top and side views (top and middle), stacking of the grid-type networks (bottom).

Cu, or Pd; Figure 3). Indeed, whereas for compounds **8** (Figure 3, bottom left) and **10** (Figure S2), a regular staggered arrangement, as presented in Figure 4b, is observed, four consecutive staggered grids form the repeating stacking unit, for the CuCdMOF **9** (Figure 3, bottom center). For PdCdMOF **11** (Figure 3, bottom right), consecutive grids are arranged with a regular offset between them. These variations emphasize the influence of the primary metal cation M on the structure of the grids and their arrangement in the crystalline state. Furthermore, the impact of the solvent employed for the

dx.doi.org/10.1021/ic402892f | *Inorg. Chem.* 2013, 52, 14439−14448

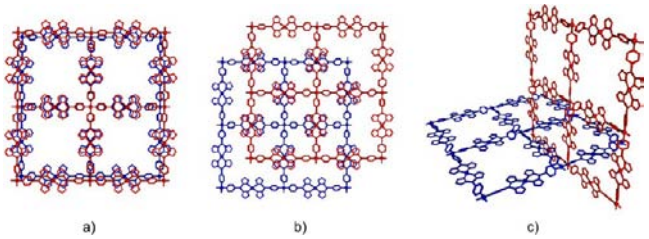

Figure 4. Schematic representations of possible packing arrangements of the 2D grid-type networks in the crystal: eclipsed (a), staggered stacking (b), and 2-fold interpenetrated (c). For sake of clarity, only the pyridyl appended tecton was chosen for the illustration.

synthesis is clearly highlighted when comparing the way these 2D networks stack in the crystal for CuCdMOFs **9** and **10** (Figure 3 and Figure S2) prepared under different conditions. The 3D packing observed leads to different solvent accessible voids, as calculated by PLATON:[18] 49% for **8**, 46.8% for **9**, 43.8% for **10**, and 34.5% for **11**. The thermal behavior of MCdMOFs **8**–**11** was investigated by TGA (Figure S3). For these compounds, a weight loss of 27.3, 19.1, 13.3, and 24.5% occurs respectively between 25 and 200 °C, corresponding to the evacuation of solvent molecules included in the structure. A plateau is then observed before decomposition of the products in the 270–300 °C temperature range.

Regarding the architectures based on tecton **2**, a dpm unit appended with an imidazole moiety, the presence of different possible rotamers should be considered, owing to the rotational freedom around the σ bond between the phenyl spacer and the peripheral imidazolyl group. Thus, depending on the orientation of the peripheral N atom of the two imidazolyl groups in the Zn(II) and Pd(II) metallatectons **6** and **7** (Scheme 1), these complexes may adopt different mutual orientations ranging from the *syn* to *anti* disposition. One may therefore envision the invariance of the connectivity pattern leading to grid-type assemblies, however with rhombic geometry of different sizes, shapes, and organization in the crystalline state.

Single crystals of ZnCdMOF **12** ($[\mathbf{6}]_2CdCl_2(DMF)$, Figure 5, left) were obtained by diffusion of a solution of $CdCl_2$ in MeOH into a DMF solution of **6**. Similar reaction with the Pd(II) metallatecton **7** in $CHCl_3$ led to the formation of PdCdMOF **13** ($[\mathbf{7}]_2CdCl_2(CHCl_3)$, Figure 5, right). For both structures, owing to the important positional disorder of solvent molecules, the corresponding electron density was again treated with the SQUEEZE command.[18] As for the pyridyl-based compounds **8**–**11** described above, the Cd(II) center is in an octahedral coordination environment with two chloride anions in apical positions and four imidazolyl groups belonging to four metallatectons (Table 1, Figure 5) leading to rhombic grid-type networks. The side of a rhombus is 26.50- and 25.30-Å-long for **12** and **13**, respectively. These values are higher than the metal–metal distance of *ca.* 20 Å observed for compounds **8**–**11**, as a result of the presence of a phenyl spacer between the dpm chelate and the peripheral imidazolyl unit in **2**. In contrast to the structure of the discrete starting species **6**, the Zn(II) cation in **12** adopts a tetrahedral environment with a C_5–Zn–$C_{5'}$ angle of 176.7°. As observed for **7**, the Pd complex

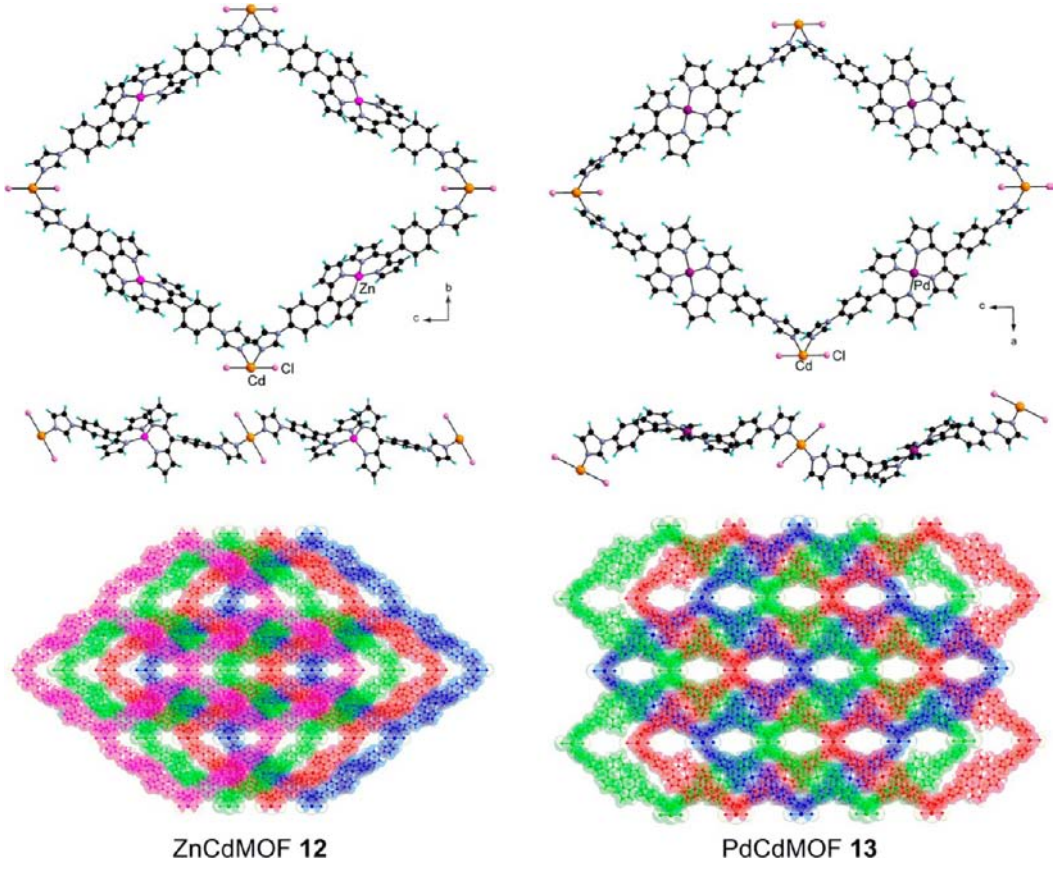

Figure 5. Portions of crystal structure of ZnCdMOF **12** and PdCdMOF **13**. Top and side views (top and middle), stacking or interpenetration of the grid-type networks (bottom).

dx.doi.org/10.1021/ic402892f | *Inorg. Chem.* 2013, 52, 14439–14448

is square planar with noncoplanar pyrrolic rings within a dpm chelate (27.9 and 34.5° for the two crystallographically independent ligands). It is worth noting that the metallatectons **6** and **7** differ not only by the coordination environment around the primary metal center M but also by the orientation of the coordinating nitrogen atom of the two imidazolyl moieties. Indeed, they are in an *anti* orientation in **12** and a *syn* orientation in **13** (Figure 5). As reported for the Cu(II) analogue,[7] consecutive grids for ZnCdMOF **12** stack with an offset, forming channels along the *c* axis (Figure 5, left). Contrastingly, in the case of **13**, a 3-fold interpenetration is observed (Figure 5, right). As a consequence of the different packing in the crystal and, in particular, as a result of the interpenetration,[1a,19] the solvent-accessible void is larger for **12** (30.9%) than for **13** (18.7%), as calculated using the PLATON sofware.[18] The thermal behavior of both MCdMOFs studied by TGA (Figure S3) indicated a weight loss of 11.0 and 10.7% for **12** and **13**, respectively, corresponding to solvent molecules present in the structure. A plateau between 150 and 300 °C is present before decomposition of products occurs.

The formation of architectures described above clearly demonstrates that the sequential strategy is viable and efficient for the generation of grid-type heterobimetallic MM′MOFs using combinations of different metallatectons (Zn(II), Cu(II), or Pd(II)) based either on the pyridyl-appended dipyrrin **1** or on imidazolyl bearing ligand **2** with $CdCl_2$. It is important to notice that, owing to the proper differentiation of the two coordinating poles and consequently the stability of $M(dpm)_2$ metallatectons, no metal exchange between the $M(dpm)_2$ complexes and $CdCl_2$ takes place preventing scrambling of M and M′ metal centers. This is further supported by the fact that $Cd(dpm)_2$ complexes based on ligands **1** and **2** have been shown to self-assemble into homometallic MOFs preventing the *in situ* formation of soluble metallatectons and hence of CdMMOFs.[21]

Paralleling the photophysical properties of their BODIPY boron analogues, metal dipyrrin complexes have also been investigated for their luminescence.[20] However, only few polymeric architectures showing emission properties have been reported.[21−24] The metallatectons **3** and **6** as well as the corresponding ZnCdMOFs **8** and **12** have been found to be luminescent in the crystalline state (Figure S4), albeit with a poor emission quantum yields of less than 1%.

One Pot Synthesis of Grid-Type MM′MOFs. Considering as reference systems the above-mentioned heterobimetallic MM′MOFs **8**−**13** generated through sequential strategy, their preparation by direct combinations of the organic tecton **1** or **2** with both metal salts was explored in a one-pot process. This approach was addressed by the slow diffusion of a MeOH solution of $CdCl_2$ and $M(OAc)_2$ (M = Zn(II), Cu(II), or Pd(II)) into a solution of either tecton **1** or **2** in DMF, $CHCl_3$, or CH_2Cl_2. Comparison of the simulated X-ray powder patterns from single-crystal data of the corresponding MCdMOFs with collected ones on crystalline materials prepared by both sequential and one-pot methods demonstrated the formation of the same crystalline materials as illustrated in Figure 6 for the two Pd(II) based PdCdMOFs **11** and **13** and in Figure S5 for the other compounds. In some cases, in particular for the Cu(II) based systems **9** and **10**, a rapid desolvation of the crystals upon removal from the mother liquor is observed. Therefore, whereas the PXRD patterns collected on different batches of **9** and **10** prepared by the stepwise and by the one-pot strategies match, they differ from the simulated ones from the single crystal data. Furthermore, in the case of **10** obtained from the CH_2Cl_2/MeOH solvent system, the PXRD investigation showed broad peaks indicating a loss of crystallinity. However, structure determination on a single crystal obtained by the one-pot approach confirmed that the MCdMOFs generated by both strategies were identical. Finally, the already reported[7] CuCdMOF based on the combination of dpm **2**, Cu(II), and $CdCl_2$ has been also successfully prepared using the one-pot method (Figure S6). Furthermore, the same reaction with $CuCl_2$ instead of $Cu(OAc)_2$ also leads to the same CuCdMOF, highlighting the selectivity of the two coordination sites for a given metal cation (dpm moiety for Cu(II) and imidazolyl unit for Cd(II)) even when these metal cations are introduced as chloride salts.

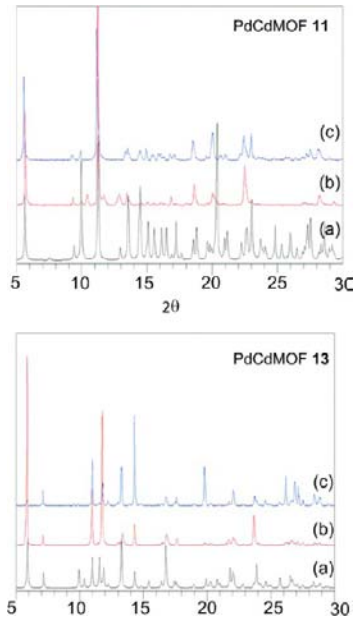

Figure 6. PXRD patterns simulated from single-crystal data (a) and experimentally obtained on crystalline material prepared by the sequential (b) or one-pot (c) method for **11** (top) and **13** (bottom). Differences in intensity arise from preferential orientation.

Although the detailed mechanism of the formation of these MM′MOFs remains undefined, owing to the relative affinity of the coordination sites for the metal salts employed and the different stability of the $M(dpm)_2$ (M = Zn, Cu, Pd) and $Cd(dpm)_2$ complexes,[21,25] it seems reasonable to propose a scenario based on the *in situ* generation of the same metallatectons as those used in the sequential approach, followed by their bridging by $CdCl_2$ behaving as tetracoordinated nodes.

It should be emphasized that this one-pot approach is *per se* easier to implement than the stepwise one, since it does not require the isolation and characterization of the metallatecton. Furthermore, for metallatectons only slightly soluble in common organic solvents such as the Pd species **5** and **7**, the sequential strategy requires the use of a larger volume of solvents, making the one-pot alternative even more attractive.

■ CONCLUSION

Dipyrrin derivatives appended with either a pyridyl or a phenylimidazolyl moiety were conceived as differentiated ditopic tectons for the preparation of a series of grid-type mixed metal−organic frameworks (MM′MOFs) following two strat-

dx.doi.org/10.1021/ic402892f | Inorg. Chem. 2013, 52, 14439−14448

egies: a sequential approach and a one-pot process. These two synthetic methods rely on the differentiation of the two coordination sites (dpm vs peripheral group) based on their charge (monoanionic vs neutral) and denticity (chelate vs monodentate) and their different affinity for the metal salts employed. For the sequential strategy, five discrete Zn(II), Cu(II), and Pd(II) metallatectons have been prepared and characterized both in solution and in the solid state by X-ray diffraction on single crystals. All five species have been subsequently combined with $CdCl_2$ to form MM′MOFs. In these architectures, four metallatectons bridge consecutive Cd(II) cations, adopting an octahedral coordination environment with two additional chloride anions in apical positions, leading to similar grid-type arrangements. The shape of the rhombus defining these grids as well as the way these stack/interpenetrate were found to be dependent on the nature of the metallatecton and the solvent. In particular, whereas the Cu(II) and Zn(II) based complexes lead to grids with a rather flat shape, ruffled arrangements are observed for the Pd(II) species. Therefore, although displaying the same type of connectivity, these heterometallic porous crystalline materials offer diverse solvent accessible voids.

The preparation of these MM′MOFs was also investigated by a one-pot strategy through combinations of dipyrrin based ligands with metal salts. Interestingly, this one-pot procedure leads to the same architectures, as demonstrated by X-ray diffraction on single-crystals and on microcrystalline powders. This straightforward approach is efficient and considerably more convenient than the sequential alternative, since it does not require the synthesis, isolation, purification, and characterization of the, sometimes insoluble, metallatectons. It should be emphasized that the stepwise strategy relies on the assembly of two components (the metallatecton and $CdCl_2$) besides the solvent molecules, whereas the one-pot approach relies on the self-assembly of the dipyrrin derivative, $M(OAc)_2$, and $CdCl_2$. In spite of the involvement of more components, the direct approach produces the same MM′MOFs, thus highlighting the specifically programmed nature of the different building units involved in the assembly process.

This direct synthetic strategy appears as an efficient and thus promising alternative to the, otherwise largely explored, stepwise approach and may be applied to other combinations of differentiated tectons and metal centers or metal complexes. We are currently investigating the scope of the one-pot construction of other MM′MOFs using different dipyrrins as well as other ligands and metal salts.

EXPERIMENTAL SECTION

Synthesis. Dipyrrins **1** and **2** and Cu(II) complex **4** were prepared as described.[5,6c,10] Since, in the reported procedure,[11] the Zn(II) compound **3** is obtained as a mixture with ligand **1**, a modified synthesis was developed. All other reagents are commercially available and were used as received. All MM′MOFs were prepared by the liquid−liquid diffusion technique at room temperature. ^1H and ^{13}C NMR spectra were recorded at 25 °C on a Bruker AV300 (300 MHz) or AV500 (500 MHz) with the deuterated solvent as the internal reference. NMR chemical shifts and J values are given in parts per million (ppm) and in Hertz, respectively. Elemental analyses were performed by the service commun d′analyses (University of Strasbourg). For compounds **8**, **9**, **12**, and **13**, the nature and number of solvent molecules present in the crystal could not be accurately determined, owing to the high positional disorder and the subsequent use of the SQUEEZE command during the crystal structure determination (see below). Therefore, no yield is given for the synthesis of these MM′MOFs.

Complex ***3***. To a solution of **1** (500 mg, 2.25 mmol) in $CHCl_3$ (60 mL) were added NEt_3 (1 mL) and a solution of $ZnCl_2$ (154 mg, 1.12 mmol) in MeOH (50 mL). The mixture was stirred overnight at RT. The solution was then concentrated (5 mL) to afford an orange crystalline powder. Rinsing with Et_2O afforded **3** as an orange solid (513 mg, 90%). ^1H NMR (300 MHz, $CDCl_3$): 6.44 (dd, J = 1.3 and 4.2 Hz, 4H), 6.64 (dd, J = 0.9 and 4.2 Hz, 4H), 7.51 (dd, J = 1.5 and 4.4 Hz, 4H), 7.57−7.58 (m, 4H), 8.75 (dd, J = 1.5 and 4.4 Hz, 4H). ^{13}C NMR (75 MHz, $CDCl_3$): 118.0, 125.4, 132.7, 139.6, 145.0, 147.1, 149.1, 150.8. Anal. Calcd. for $C_{28}H_{20}N_6Zn$: C, 66.48; H, 3.98; N, 16.61. Found: C, 66.52; H, 3.97; N, 16.43. Single crystals were obtained by *n*-pentane vapor diffusion into a solution of the complex in dioxane.

Complex ***5***. A solution of $Pd(OAc)_2$ (19.5 mg, 0.11 mmol) in MeOH (10 mL) is added to a solution of **1** (50 mg, 0.22 mmol) in $CHCl_3$. Following the addition of NEt_3 (1 mL), the solution was stirred at RT for 4 h. After evaporation, the addition of MeOH afforded **5** as a red crystalline precipitate (44.9 mg, 74%). ^1H NMR (500 MHz, $CDCl_3$): 6.40 (d, J = 4.2 Hz, 4H), 6.65 (d, J = 4.4 Hz, 4H), 7.42 (br s, 4H), 7.52 (d, J = 4.9 Hz, 4H), 8.77 (d, J = 5.0 Hz, 4H). ^{13}C NMR (125 MHz, $CDCl_3$): 117.7, 125.0, 130.1, 136.1, 144.1, 145.4, 149.2, 152.5. MS (MALDI) m/z: 547.04 [M + H] (calcd. 547.09). UV−vis ($CHCl_3$) λ_{max} (nm)/ε (M^{-1} cm^{-1}): 311 (8200), 397 (12 950), 485 (64 400). Single crystals were obtained by slow diffusion of a MeOH solution of $Pd(OAc)_2$ in a DMF solution of **1**.

Complex ***6***. A solution of $ZnCl_2$ (47.6 mg, 0.35 mmol) in MeOH (25 mL) was added to a solution of **2** (200, 0.70 mmol) in $CHCl_3$ (25 mL). Following the addition of NEt_3 (0.8 mL), the solution was agitated at RT for 64 h. Upon concentration of the solution (15 mL), an orange precipitate was formed which was filtered, washed with MeOH, then dried to afford complex **6** (187 mg, 84%). ^1H NMR (500 MHz, $CDCl_3$): 6.46 (dd, J = 1.2 and 4.2 Hz, 4H), 6.75 (dd, J = 4.2 and 0.9 Hz, 4H), 7.22−7.23 (m, 2H), 7.44−7.45 (m, 2H), 7.54−7.58 (m, 8H), 7.68−7.72 (m, 4H), 8.00 (s, 2H). ^{13}C NMR (125 MHz, $CDCl_3$): 117.8, 118.5, 120.5, 130.9, 132.6, 133.2, 136.0, 138.1, 138.5, 140.9, 147.7, 150.3. HRMS (ESI) m/z: 635.164 $[M + H]^+$ (calcd. 635.164). UV−vis ($CHCl_3$) λ_{max} (nm)/ε (M^{-1} cm^{-1}): 342 (19 200), 470 (72 900), 487 (118 000). Single crystals were obtained by Et_2O vapor diffusion into a solution of the complex in $CHCl_3$.

Complex ***7***. A solution of $Pd(OAc)_2$ (52 mg, 0.30 mmol) in MeOH (30 mL) was added to a solution of **2** (199 mg, 0.70 mmol) in $CHCl_3$. After addition of NEt_3 (1.5 mL), the solution was stirred at RT overnight. After evaporation, addition of MeOH afforded a red crystalline precipitate, recovered by centrifugation and rinsed with Et_2O to afford **7** (142 mg, 70%). The product is only slightly soluble in $CDCl_3$, preventing ^{13}C NMR data collection. ^1H NMR (500 MHz, $CDCl_3$): 6.41 (d, J = 4.3 Hz, 4H), 6.73 (d, J = 4.3 Hz, 4H),7.28−7.29 (m, 2H), 7.41−7.42 (m, 2H), 7.43−7.44 (m, 4H), 7.54 (d, J = 7.9 Hz, 4H), 7.72 (d, J = 7.9 Hz, 4H), 8.00 (s, 2H). MS (MALDI) m/z: 677.14 [M + H] (calcd. 677.14). UV−vis ($CHCl_3$) λ_{max} (nm)/ε (M^{-1} cm^{-1}): 345 (16 600), 393 (14 900), 484 (66 600). Single crystals were obtained by slow diffusion of a MeOH solution of $Pd(OAc)_2$ into a $CHCl_3$ solution of **2**.

ZnCdMOF ***8***. *Sequential Synthesis.* In a vial (Ø × h = 61 × 16 mm), a DMF (2 mL) solution of **3** (22.1 mg, 0.044 mmol) was layered with a DMF/MeOH (1/1, 1 mL) buffer, and then a MeOH (2 mL) solution of $CdCl_2$ (4 mg, 0.022 mmol) was added. After a few days, 21.8 mg of orange crystals were obtained.

One-Pot Synthesis. In a vial (Ø × h = 61 × 16 mm), a DMF (1 mL) solution of dpm **1** (9.7 mg, 0.044 mmol) was layered with a DMF/MeOH (1/1, 1 mL) buffer and topped with a mixture of $CdCl_2$ (2 mg, 0.011 mmol) and $Zn(OAc)_2$ (4.1 mg, 0.022 mmol) in MeOH (2 mL). After a few days, 4.1 mg of large single crystals were obtained.

CuCdMOF ***9***. *Sequential Synthesis.* A DMF (2 mL) solution of **4** (10 mg, 0.02 mmol) was mixed with a MeOH (2 mL) solution of $CdCl_2$ (10 mg, 0.05 mmol). Upon vapor diffusion of Et_2O, 7.1 mg of dark-red crystals were obtained.

dx.doi.org/10.1021/ic402892f | *Inorg. Chem.* 2013, 52, 14439−14448

Table 3. Crystallographic Data for MM′MOFs 8−13

	8	9	10	11	12	13
formula	$C_{56}H_{40}CdCl_2N_{12}Zn_2$	$C_{56}H_{40}CdCl_2Cu_2N_{12}$	$C_{64}H_{56}CdCl_{18}Cu_2N_{12}$	$C_{60}H_{44}CdCl_{14}N_{12}Pd_2$	$C_{75}H_{59}CdCl_2N_{17}OZn_2$	$C_{73}H_{53}CdCl_5N_{16}Pd_2$
fw	1195.04	1191.38	1870.79	1754.57	1528.43	1656.76
crystal system	tetragonal	tetragonal	tetragonal	triclinic	monoclinic	orthorhombic
space group	$P4/nnc$	$P4_322$	$I\bar{4}2m$	$P\bar{1}$	$C2/m$	$Pmn2_1$
a, Å	20.0126(3)	20.0626(4)	20.2165(5)	9.0610(2)	13.4833(8)	30.0402(11)
b, Å				11.9362(2)	31.8550(18)	8.9013(3)
c, Å	10.3775(3)	19.8105(6)	9.0878(3)	15.7702(3)	19.4871(9)	13.5698(5)
α, deg				89.5150(10)		
β, deg				85.8570(10)	95.092(2)	
γ, deg				79.4270(10)		
V, Å^3	4156.23(15)	7973.9(3)	3714.25(18)	1672.25(6)	8336.9(8)	3628.5(2)
Z	2	4	2	1	4	2
T, K	173(2)	173(2)	173(2)	173(2)	173(2)	173(2)
μ, mm^{-1}	0.922	0.893	1.548	1.456	0.937	1.018
reflns. coll.	58165	70723	21260	33517	67790	30173
ind. reflns. (R_{int})	2600 (0.0349)	9210 (0.0826)	2833 (0.0224)	8884 (0.0323)	7550 (0.0534)	9400 (0.0360)
R_1 ($I > 2\sigma(I)$)[a]	0.0350	0.0460	0.0644	0.0328	0.0654	0.0665
wR_2 ($I > 2\sigma(I)$)[a]	0.0822	0.1088	0.1782	0.0820	0.2016	0.1747
R_1 (all data)[a]	0.0452	0.0655	0.0664	0.0414	0.0860	0.0851
wR_2 (all data)[a]	0.0867	0.1153	0.1820	0.0919	0.2149	0.1839
GOF	1.037	0.998	1.130	1.069	1.078	1.059

[a] $R_1 = \sum||F_o| - |F_c||/\sum|F_o|$; $wR_2 = [\sum w(F_o^2 - F_c^2)^2/\sum wF_o^4]^{1/2}$.

One-Pot Synthesis. In a vial (Ø × h = 61 × 16 mm), a DMF (2 mL) solution of dpm **1** (19.4 mg, 0.088 mmol) was layered with a DMF/MeOH (1/1, 1 mL) buffer layer before a mixture of $CdCl_2$ (4 mg, 0.022 mmol) and $Cu(OAc)_2$ (8.8 mg, 0.044 mmol) in MeOH (4 mL) was added. After few days, 10.3 mg crystals were obtained.

*CuCdMOF **10**. Sequential Synthesis.* In a vial (Ø × h = 65 × 22 mm), a CH_2Cl_2 (5 mL) solution of **4** (22 mg, 0.044 mmol) was layered a CH_2Cl_2/MeOH (1/1, 2 mL) buffer layer before a MeOH (2 mL) solution of $CdCl_2$ (4 mg, 0.022 mmol) was added. After few days, dark-red crystals of **10** were obtained (7.3 mg, 18%).

One-Pot Synthesis. In a vial (Ø × h = 65 × 22 mm), a CH_2Cl_2 (5 mL) solution of dpm **1** (19.4 mg, 0.088 mmol) was layered with a CH_2Cl_2/MeOH (1/1, 1 mL) buffer before a mixture of $CdCl_2$ (4 mg, 0.022 mmol) and $Cu(OAc)_2$ (8.8 mg, 0.044 mmol) in MeOH (4 mL) was added. After 2 weeks, the single crystals obtained were filtered (23 mg, 56%).

*PdCdMOF **11**. Sequential Synthesis.* In a vial (Ø × h = 61 × 16 mm), a $CHCl_3$ (2 mL) solution of **5** (8 mg, 0.015 mmol) was layered with a $CHCl_3$/MeOH (1/1, 1 mL) buffer. A MeOH (2 mL) solution of $CdCl_2$ (3 mg, 0.016 mmol) was layered on top. After a few days, red crystals were obtained (8.0 mg, 57%).

One-Pot Synthesis. In a vial (Ø × h = 61 × 16 mm), a $CHCl_3$ (3 mL) solution of **1** (19.2 mg, 0.086 mmol) was first layered with a $CHCl_3$/MeOH (1/1, 1 mL) buffer before a MeOH (3 mL) solution of $CdCl_2$ (4 mg, 0.022 mmol) and $Pd(OAc)_2$ (7.7 mg, 0.043 mmol) was added. After a few days, crystals were obtained (4.5 mg, 12%).

*ZnCdMOF **12**. Sequential Synthesis.* In a vial (Ø × h = 65 × 22 mm), a DMF (4 mL) solution of **6** (20 mg, 0.03 mmol) was first layered with a DMF/MeOH (1/1, 3 mL) buffer before a MeOH (5 mL) solution of $CdCl_2$ (20 mg, 0.11 mmol) was added. After a few days, 8.6 mg of orange crystals were obtained.

One-Pot Synthesis. In a vial (Ø × h = 61 × 16 mm), a DMF (1.5 mL) solution of dpm **2** (16.3 mg, 0.057 mmol) was first layered with a DMF/MeOH (1/1, 1 mL) buffer before a MeOH (2 mL) solution of $CdCl_2$ (2.6 mg, 0.014 mmol) and $Zn(OAc)_2$ (6.2 mg, 0.028 mmol) was added. After a few days, 10.6 mg of large orange crystals were obtained.

*PdCdMOF **13**. Sequential Synthesis.* In a vial (Ø × h = 65 × 22 mm), a $CHCl_3$ (4 mL) solution of **7** (14.8 mg, 0.022 mmol) was mixed with a MeOH (4 mL) solution of $CdCl_2$ (2 mg, 0.11 mmol). After a few days, 5.2 mg of red crystals were obtained.

One-Pot Synthesis. In a test tube, a $CHCl_3$ (3 mL) solution of **2** (20 mg, 0.070 mmol) was first layered with a $CHCl_3$/MeOH (1/1, 4 mL) buffer before a MeOH (6 mL) solution of $CdCl_2$ (6.2 mg, 0.017 mmol) and $Pd(OAc)_2$ (6.2 mg, 0.035 mmol) was added. After two weeks, 11.2 mg of red crystals were obtained.

X-Ray Diffraction. Single-crystal data (Tables 2 and 3) were collected on a Bruker SMART CCD diffractometer with Mo Kα radiation. The structures were solved using SHELXS-97 and refined by full matrix least-squares on F^2 using SHELXL-97 with anisotropic thermal parameters for all non-hydrogen atoms.[26] The hydrogen atoms were introduced at calculated positions and not refined (riding model). For compounds **8**, **9**, **12**, and **13**, solvent molecules present in the structures show high positional disorder. To account for the corresponding electron density, the SQUEEZE command was used.[18] CCDC 952061−952073 contain the supplementary crystallographic data for compounds **3**−**13**. These data can be obtained free of charge *via* www.ccdc.cam.ac.uk/data_request/cif.

Powder X-ray diffraction diagrams were collected at 293 K on a Bruker D8 diffractometer using monochromatic Cu Kα radiation with a scanning range between 4 and 40° using a scan step of 2°/mn. The simulated diagrams are based on single-crystal data collected at 173 K.

Thermo-Gravimetric Analysis. Thermo-gravimetric analyses were performed on a Perkin-Elmer Pyris 6 TGA with a scan rate of 3 °C/min under a flux of nitrogen (20 mL/min).

Luminescence. Solid state measurements were performed on a Perkin-Elmer LS 55 spectrometer.

dx.doi.org/10.1021/ic402892f | *Inorg. Chem.* 2013, 52, 14439−14448

■ ASSOCIATED CONTENT

Supporting Information

Crystal data for (**5**)$(MeOH)_2$ and (**5**)$(CHCl_3)_2$, TGA curves for **8**−**13**, PXRD patterns for **8**−**11**. This material is available free of charge via the Internet at http://pubs.acs.org.

■ AUTHOR INFORMATION

Corresponding Authors

*E-mail: hosseini@unistra.fr.

*E-mail: sbaudron@unistra.fr.

Notes

The authors declare no competing financial interest.

■ ACKNOWLEDGMENTS

We thank the Université de Strasbourg, the Institut Universitaire de France, the International centre for Frontier Research in Chemistry (icFRC), the C.N.R.S., and the Ministère de l'Enseignement Supérieur et de la Recherche (Ph.D. fellowship to A.B.) for financial support. The assistance of Dr. Matteo Mauro (Université de Strasbourg) in the determination of the emission quantum yield in the solid state is gratefully acknowledged.

■ REFERENCES

(1) (a) Batten, S. R.; Robson, R. *Angew. Chem., Int. Ed.* **1998**, *37*, 1460. (b) Eddaoudi, M.; Moler, D. B.; Li, H.; Chen, B.; Reineke, T. M.; O'Keeffe, M.; Yaghi, O. M. *Acc. Chem. Res.* **2001**, *34*, 319. (c) Kitagawa, S.; Kitaura, R.; Noro, S. I. *Angew. Chem. Int. Ed.* **2004**, *43*, 2334. (d) *Chem. Soc. Rev.* **2009**, *38* (5), themed issue on metal-organic frameworks. (e) Janiak, C.; Vieth, J. K. *New J. Chem.* **2010**, *34*, 2366. (f) *Chem. Rev.* **2012**, *112* (2), 2012 Metal−Organic Frameworks special issue. (g) Wang, C.; Lin, W. *J. Am. Chem. Soc.* **2013**, *135*, 13222.

(2) (a) Simard, M.; Su, D.; Wuest, J. D. *J. Am. Chem. Soc.* **1991**, *113*, 4696. (b) Mann, S. *Nature* **1993**, *365*, 499. (c) Hosseini, M. W. *Acc. Chem. Res.* **2005**, *38*, 313. (d) Hosseini, M. W. *Chem. Commun.* **2005**, 5825.

(3) (a) Kitagawa, S.; Noro, S.; Nakamura, T. *Chem. Commun.* **2006**, 701. (b) Andruh, M. *Chem. Commun.* **2007**, 2565. (c) Garibay, S. J.; Stork, J. R.; Cohen, S. M. *Prog. Inorg. Chem.* **2009**, *56*, 335. (d) Burrows, A. D. *CrystEngComm.* **2011**, *13*, 3623. (e) Das, M. C.; Xiang, S.; Zhang, Z.; Chen, B. *Angew. Chem., Int. Ed.* **2011**, *50*, 10510. (f) Kumar, G.; Gupta, R. *Chem. Soc. Rev.* **2013**, *24*, 9403.

(4) (a) Wood, T. E.; Thompson, A. *Chem. Rev.* **2007**, *107*, 1831. (b) Maeda, H. *Eur. J. Org. Chem.* **2007**, 5313. (c) Baudron, S. A. *CrystEngComm* **2010**, *12*, 2288.

(5) (a) Halper, S. R.; Cohen, S. M. *Inorg. Chem.* **2005**, *44*, 486. (b) Murphy, D. L.; Malachowski, M. R.; Campana, C. F.; Cohen, S. M. *Chem. Commun.* **2005**, 5506. (c) Halper, S. R.; Do, L.; Stork, J. R.; Cohen, S. M. *J. Am. Chem. Soc.* **2006**, *128*, 15255. (d) Stork, J. R.; Thoi, V. S.; Cohen, S. M. *Inorg. Chem.* **2007**, *46*, 11213. (e) Garibay, S.; Stork, J. R.; Wang, Z.; Cohen, S. M.; Telfer, S. G. *Chem. Commun.* **2007**, 4881.

(6) (a) Salazar-Mendoza, D.; Baudron, S. A.; Hosseini, M. W. *Chem. Commun.* **2007**, 2252. (b) Salazar-Mendoza, D.; Baudron, S. A.; Hosseini, M. W. *Inorg. Chem.* **2008**, *47*, 766. (c) Pogozhev, D.; Baudron, S. A.; Hosseini, M. W. *Inorg. Chem.* **2010**, *49*, 331. (d) Kilduff, B.; Pogozhev, D.; Baudron, S. A.; Hosseini, M. W. *Inorg. Chem.* **2010**, *49*, 11231. (e) Béziau, A.; Baudron, S. A.; Hosseini, M. W. *Dalton Trans.* **2012**, *41*, 7227.

(7) Béziau, A.; Baudron, S. A.; Pogozhev, D.; Fluck, A.; Hosseini, M. W. *Chem. Commun.* **2012**, *48*, 10313.

(8) (a) Fujita, M.; Kwon, Y. J.; Washizu, S.; Ogura, K. *J. Am. Chem. Soc.* **1994**, *116*, 1151. (b) Abrahams, B. F.; Hoskins, B. F.; Robson, R.; Slizys, D. A. *CrystEngComm* **2002**, *4*, 478. (c) Davidson, G. J. E.; Loeb, S. J. *Angew. Chem., Int. Ed.* **2003**, *42*, 74. (d) Zhu, H.-F.; Zhao, W.; Okamura, T.; Fan, J.; Sun, W.-Y.; Ueyama, N. *New J. Chem.* **2004**, *28*, 1010. (e) Wu, C.-D.; Hu, A.; Zhang, L.; Lin, W. *J. Am. Chem. Soc.* **2005**, *127*, 8940. (f) Plater, M. J.; Gelbrich, T.; Hursthouse, M. B.; De Silva, B. M. *CrystEngComm.* **2006**, *C*, 895. (g) Zheng, S.-R.; Yang, Q.-Y.; Liu, Y.-R.; Zhang, J.-Y.; Tong, Y.-X.; Zhao, C.-Y.; Su, C.-Y. *Chem. Commun.* **2008**, 356−358. (h) Constable, E. C.; Zhang, G.; Housecroft, C. E.; Neuburger, M.; Zampese, J. A. *CrystEngComm.* **2009**, *11*, 2279.

(9) (a) Chen, B.; Fronczek, F. R.; Maverick, A. W. *Inorg. Chem.* **2004**, *43*, 8209. (b) Vreshch, V. D.; Lysenko, A. B.; Chernega, A. N.; Howard, J. A. K.; Krautscheid, H.; Sieler, J.; Domasevitch, K. V. *Dalton Trans.* **2004**, 2899. (c) Deiters, E.; Bulach, V.; Hosseini, M. W. *New J. Chem.* **2006**, *30*, 1289. (d) Vreshch, V. D.; Lysenko, A. B.; Chernega, A. N.; Sieler, J.; Domasevitch, K. V. *Polyhedron* **2008**, *24*, 917. (e) Deiters, E.; Bulach, V.; Hosseini, M. W. *New J. Chem.* **2008**, *32*, 99. (f) Zou, C.; Zhang, Z.; Xu, X.; Gong, Q.; Li, J.; Wu, C.-D. *J. Am. Chem. Soc.* **2012**, *134*, 87.

(10) Littler, B. J.; Miller, M. A.; Hung, C.-H.; Wagner, R. W.; O'Shea, D. F.; Boyle, P. D; Lindsey, J. S. *J. Org. Chem.* **1999**, *64*, 1391.

(11) (a) Wood, T. E.; Berno, B.; Beshara, B. S.; Thompson, A. *J. Org. Chem.* **2006**, *71*, 2964. (b) Maeda, H.; Hashimoto, T.; Fujii, R.; Hasegawa, M. *J. Nanosci. Nanotechnol.* **2009**, *9*, 240.

(12) Halper, S. R.; Malachowski, M. R.; Delaney, H. M.; Cohen, S. M. *Inorg. Chem.* **2004**, *43*, 1242.

(13) Hall, J. D.; McLean, T. M.; Smalley, S. J.; Waterland, M. R.; Telfer, S. G. *Dalton Trans.* **2010**, *39*, 437.

(14) (a) Yu, L.; Muthukumaran, K.; Sazanovich, I. V.; Kirmaier, K.; Hindin, E.; Diers, J. R.; Boyle, P. D.; Bocian, D. F.; Holten, D.; Lindsey, J. S. *Inorg. Chem.* **2003**, *42*, 6629. (b) Maeda, H.; Hashimoto, T. *Chem.—Eur. J.* **2007**, *13*, 7900. (c) Baudron, S. A.; Salazar-Mendoza, D.; Hosseini, M. W. *CrystEngComm.* **2009**, *11*, 1245. (d) Pogozhev, D.; Baudron, S. A.; Hosseini, M. W. *CrystEngComm.* **2010**, *12*, 2238. (e) Shin, J.-Y.; Patrick, B. O.; Son, S. B.; Hahn, J. R.; Dolphin, D. *Bull. Chem. Soc. Kor.* **2010**, *31*, 1004. (f) Hashimoto, T.; Nishimura, T.; Lin, J. M.; Khim, D.; Maeda, H. *Chem.—Eur. J.* **2010**, *16*, 11653. (g) Artigau, M.; Bonnet, A.; Ladeira, S.; Hoffmann, P.; Vigroux, A. *CrystEngComm.* **2011**, *13*, 7149. (h) Maeda, H.; Nishimura, T.; Akuta, R.; Takaishi, K.; Uchiyama, M.; Muranaka, A. *Chem. Sci.* **2013**, *4*, 1204. (i) Maeda, H.; Akuta, R.; Bando, Y.; Takaishi, K.; Uchiyama, M.; Muranaka, A.; Tohnai, N.; Seki, S. *Chem.—Eur. J.* **2013**, *19*, 11676.

(15) (a) Halper, S. R.; Cohen, S. M. *Chem.—Eur. J.* **2003**, *9*, 4661. (b) Do, L.; Halper, S. R.; Cohen, S. M. *Chem. Commun.* **2004**, 2662. (c) Miao, Q.; Shin, J.-Y.; Patrick, B. O.; Dolphin, D. *Chem. Commun.* **2009**, 2541. (d) Yadav, M.; Kumar, P.; Singh, A. K.; Ribas, J.; Pandey, D. S. *Dalton Trans.* **2009**, 9929. (e) Toganoh, M.; Gokulnath, S.; Kawabe, Y.; Furuta, H. *Chem.—Eur. J.* **2012**, *18*, 4380.

(16) Bronner, C.; Baudron, S. A.; Hosseini, M. W.; Strassert, C. A.; Guenet, A.; De Cola, L. *Dalton Trans.* **2010**, *39*, 180.

(17) Béziau, A.; Baudron, S. A.; Rogez, G.; Hosseini, M. W. *CrystEngComm.* **2013**, *15*, 5980.

(18) Spek, A. L. *PLATON*; The University of Utrecht: Utrecht, The Netherlands, 1999.

(19) (a) Carlucci, L.; Ciani, G.; Proserpio, D. M. *Coord. Chem. Rev.* **2003**, *246*, 247. (b) Leong, W. L.; Vittal, J. J. *Chem. Rev.* **2011**, *111*, 688. (c) Alexandrov, E. V.; Blatov, V. A.; Proserpio, D. M. *Acta Crystallogr.* **2012**, *A68*, 484. (d) Yang, G.-P.; Hou, L.; Luan, X.-J.; Wu, B.; Wang, Y.-Y. *Chem. Soc. Rev.* **2012**, *41*, 6992. (e) Jiang, H.-L.; Makal, T. A.; Zhou, H.-C. *Coord. Chem. Rev.* **2013**, *257*, 2232.

(20) Baudron, S. A. *Dalton Trans.* **2013**, *42*, 7498.

(21) Béziau, A.; Baudron, S. A.; Guenet, A.; Hosseini, M. W. *Chem.—Eur. J.* **2013**, *19*, 3215.

(22) (a) Maeda, H.; Hasegawa, M.; Hashimoto, T.; Kakimoto, T.; Nishio, S.; Nakanishi, T. *J. Am. Chem. Soc.* **2006**, *128*, 10024. (b) Maeda, H.; Kobayashi, H.; Akuta, R. *J. Porphyrins Phthalocyanines* **2013**, *17*, 86.

(23) Kobayashi, J.; Kushida, T.; Kawashima, T. *J. Am. Chem. Soc.* **2009**, *131*, 10836.

(24) (a) Lee, C. Y.; Farha, O. K.; Hong, B. J.; Sarjeant, A. A.; Nguyen, S. T.; Hupp, J. T. *J. Am. Chem. Soc.* **2011**, *133*, 15858. (b) Zhou, L.; Xue, Y. S.; Xu, Y.; Zhang, J.; Du, H.-B. *CrystEngComm* **2013**, *15*, 7315.
(25) Guseva, G. B.; Antina, E. V.; Berezin, M. B.; V'yugin, V. *Russ. J. Coord. Chem.* **2004**, *30*, 32.
(26) Sheldrick, G. M. *Acta Crystallogr.* **2008**, *A64*, 112.